

Characterization of Different Chemical Blowing Agents and Their Applicability to
Produce Poly(Lactic Acid) Foams by Extrusion

Kmetty Á., Litauszki K., Réti D.

Accepted for publication in Applied Sciences

Published in 2018

DOI: [10.3390/app8101960](https://doi.org/10.3390/app8101960)

Article

Characterization of Different Chemical Blowing Agents and Their Applicability to Produce Poly(Lactic Acid) Foams by Extrusion

Ákos Kmetty ^{1,2,*} , Katalin Litauszki ¹  and Dániel Réti ¹

¹ Department of Polymer Engineering, Faculty of Mechanical Engineering, Budapest University of Technology and Economics, Műgyetem rkp. 3., H-1111 Budapest, Hungary; litauszkik@pt.bme.hu (K.L.); reti.daniel92@gmail.com (D.R.)

² MTA–BME Research Group for Composite Science and Technology, Műgyetem rkp. 3., H-1111 Budapest, Hungary

* Correspondence: kmetty@pt.bme.hu; Tel.: +36-1-463-2004

Received: 25 September 2018; Accepted: 11 October 2018; Published: 17 October 2018



Abstract: This study presents the applicability of different types (exothermic and endothermic) of chemical blowing agents (CBAs) in the case of poly(lactic acid) (PLA). The amount of foaming agent is a fixed 2 wt%. We used a twin-screw extruder and added the individual components in the form of dry mixture through the hopper of the extruder. We characterized the PLA matrix and the chemical blowing agents with different testing methods. In case of the produced foams we carried out morphological and mechanical tests and used scanning electron microscopy to examine cell structure. We showed that PLA can be successfully foamed with the use of chemical blowing agents. The best results were achieved with an exothermic CBA and with PLA type 8052D. The cell population density of PLA foams produced this way was 4.82×10^5 cells/cm³, their expansion was 2.36, their density 0.53 g/cm³ and their void fraction was 57.61%.

Keywords: chemical blowing agent; poly(lactic acid) foam; foam extrusion

1. Introduction

Nowadays the number and amount of polymers produced from renewable resources are increasing considerably. These polymers are also readily available [1]. Global market forecasts predict a fourfold increase until 2019 (7.8 million ton/year) [2]. Polymer foams nowadays are mostly produced from petroleum-based materials. Foamed products, made by physical [3], chemical [4] and bead foaming techniques [5], in addition there are innovative examples of metallic foams as well [6]. Although physical foaming technique produce a lower foam density (density reduction up to 80%), chemical foaming agents can be used without modifying the extruder [7]. Foaming can be divided into four sections. In the initial phase, the gas enters the polymer matrix and the two phases mix. In the next section, the matrix material is saturated with the foaming gas at an elevated temperature and pressure. In the third section, the homogeneous system expands as the pressure decreases. In the final section, the structure stabilizes [8]. An important foaming method is chemical foaming, when the foaming agent requires certain conditions to decompose and in the process a gas phase is generated as a result of a chemical change. It is important to choose the decomposition temperature range of the foaming agent to match the processing temperature of the matrix polymer. Chemical blowing agents can be used in different temperature ranges. Their decomposition products are various gases. The most important is the gas that is produced in the largest quantity [9]. Foaming agents can be endothermic and exothermic. The most often used exothermic foaming agent is azodicarbonamide (ADCA), even though ADCA decomposes at a relatively high temperature, at 230 °C. When 5% 4,4'-oxybis

(benzenesulfonylhydrazide) (OBSH) is added, it reduces the initial temperature of decomposition to 205 °C. However, this temperature is still higher than the processing temperature of some very common polymers (e.g., P-PVC, U-PVC, EVA and PLA). With the use of activators (zinc stearate, zinc oxide, naphthenate, urea or benozate), the decomposition temperature range can be reduced to as low as 40 °C. The decomposition process typically yields 220 cm³/g gas. Its decomposition products are nitrogen (N₂) 65%, carbon monoxide (CO) 24%, carbon dioxide (CO₂) 5% and ammonia (NH₃) 5% [10,11]. It can produce larger cells, greatly reduce density from 1.24 g/cm³ to 0.599 g/cm³ (in case of neat, extruded PLA) but the yellowish colour of the foaming agent affects the colour of the product [12]. The most often used endothermic foaming agent is a mixture of sodium bicarbonate and citric acid. It is typically whitish, can produce finer cells and less reduction in density from 1.24 g/cm³ to 0.645 g/cm³ in case of neat, extruded PLA [12–16]. Sodium bicarbonate starts to decompose at around 160 °C, while citric acid only starts decomposing at around 210 °C. About 120 cm³/g of gas is produced. Foaming agents working in different temperature ranges can be produced by mixing the two components at different ratios [17,18]. Such CBAs typically have water among their decomposition products. If the polymer matrix is sensitive to moisture (e.g., polycarbonates or polyesters), a CBA should be chosen which does not have water among its decomposition products (or only a very small amount) because the water can hydrolyse the polymer [9].

A great disadvantage of petroleum-based polymeric materials and products made from them is that they are difficult and costly to recycle, cannot be decomposed biologically and are a considerable load on the environment after they lose their function. Renewable resource-based and biodegradable polymers offer an environmentally friendly alternative. Of all biopolymers, poly(lactic acid) (PLA) receives the most attention nowadays [19]. PLA can be foamed in many ways (extrusion foaming, foam injection moulding, bead foaming) but currently the application of supercritical fluid state carbon dioxide receives the most attention [20,21].

Foaming this biopolymer with chemical blowing agents is not fully researched yet. Commercially available CBAs are mostly designed for the foaming of petroleum-based polymers and their applicability with biodegradable polymers needs more research [22]. Our goal was to analyse a wide range of commercially widely available conventional exothermic and endothermic foaming agents so we selected two endothermic, one exothermic CBAs recommended for polyesters and a new endothermic CBA specially designed for the foaming of PLA. Such a CBA, especially recommended for PLA, has never been examined in the literature. We characterized these CBAs and investigated their applicability for PLA in detail, using continuous extrusion as manufacturing technology.

2. Materials and Methods

2.1. Material

We used poly(lactic acid) type 2003D (4.3 mol% D-lactide content) and 8052D (4.5 mol% D-lactide content), (Ingeo™ Biopolymer, NatureWorks© LLC, Minnetonka, MN, USA). The PLAs have a melting temperature of 150.9 °C and of 153.3 °C (determined by DSC from the first melting curve, 5 °C/min), a Melt Flow Index of 2 g/10 min and 7 g/10 min (CEAST 7027.000, 2.16 kg, 190 °C), respectively, as measured by the authors. The number average molecular weight was 100,422 Da, the weight average molecular weight was 180,477 Da, the polydispersity index was 1.79, the number average molecular weight was 85,562 Da, the weight average molecular weight 153,235 Da and the polydispersity index was 1.79 (Figure 1, determined by gel permeation chromatography (GPC) measurements).

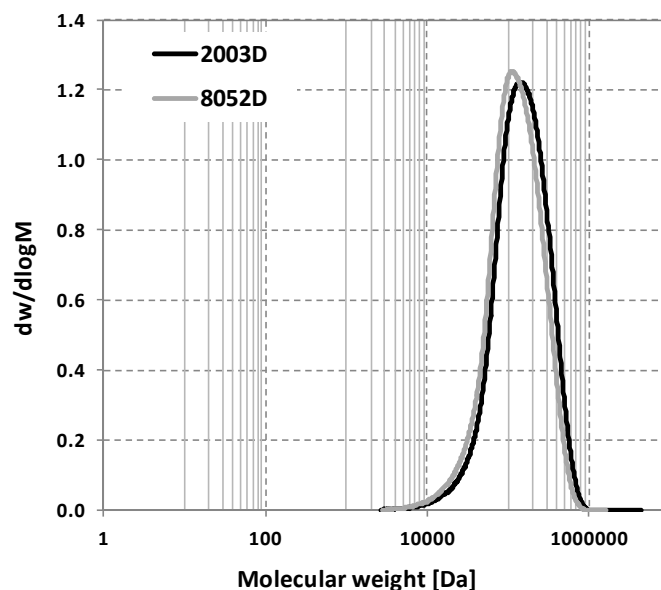


Figure 1. The molecular weight distribution of different poly(lactic acid) (PLA) granules based on a gel permeation chromatography (GPC) test.

We used exothermic and endothermic CBAs in 2 wt% for the extrusion foaming of PLA. Table 1 contains the exact types and their specifications as found on their datasheets.

Table 1. Chemical blowing agents (CBAs) used and their properties.

CBA Trade Name	Type of CBA	Blowing Agent *	Effective Gases *	Other Information *	Abbreviation
Tracel IM 3170 MS	exothermic	azodicarbonamide	N ₂ , CO, CO ₂ , NH ₃	-	Tracel3170
Tracel IMC 4200	endothermic	citric acid and baking soda	CO ₂ , H ₂ O	water is formed, it contains a nucleating agent recommended for PLA	Tracel4200
Hydrocerol CT 3168	endothermic	n.d.	n.d.		Hyd_3168
Luvobatch PE BA 9537	endothermic	n.d.	n.d.	carrier PE	Luv_9537

*—Information from Technical Datasheet, n.d.—no data from the manufacturer.

2.2. Testing Methods

2.2.1. Gel Permeation Chromatography (GPC)

The tests were performed on an Agilent PL-GPC 50 System (Santa Clara, CA, USA) GPC/SEC device. The samples were first dissolved in chloroform (ca. 30 mg/mL), then filtered through a PTFE filter. Four Agilent PL-Gel columns (3 × PL-Gel Mixed C (5 μm) and 1 × PL-Gel Mixed E (3 μm) columns) were used in series, with HPLC grade chloroform (amylene-stabilised) as the eluent, at a flow rate of 1 mL min⁻¹ at 30 °C, on a Waters Alliance system equipped with an Alliance 2695 Separation Module. The polymer number-average molecular weight (M_n) and polydispersity index (M_w/M_n ; PDI) were calibrated against low dispersity polystyrene standards with a 3rd order polynomial fit, linear across molar mass ranges.

2.2.2. Differential Scanning Calorimetry (DSC) for Chemical Blowing Agents

Differential scanning calorimetry (DSC) measurements of chemical blowing agents were performed with a Setaram DSC 92 (Caluire, France) device. The measurement temperature range was 25–250 °C, the heating rate was 10 °C/min, the mass of the samples was between 3 mg and 6 mg

and the tests were performed in nitrogen protective gas (20 mL/min) and with a nitrogen measuring atmosphere (20 mL/min).

2.2.3. Differential Scanning Calorimetry (DSC) for Biopolymer Foams

Differential scanning calorimetry (DSC) measurements of biopolymer foams were carried out with a TA Instruments Q2000 (New Castle, DE, USA) automatic sampling device. The measurement temperature range was 0–200 °C, the heating rate was 5 °C/min, the mass of the samples was between 3 mg and 6 mg and the tests were performed in nitrogen protective gas (20 mL/min) and with a nitrogen measuring atmosphere (20 mL/min). The degree of crystallinity (χ_c) was calculated according to Equation 1, where ΔH_m is the crystallization enthalpies. The degree of crystallinity (χ_{cf}) created via foam processing was calculated according to Equation (2), where ΔH_m is the melt and ΔH_c is the crystallization enthalpy. PLA_{100%} is the theoretical melting enthalpy of 100% crystalline PLA, which is 93 J/g [23].

$$\chi_c = \frac{\Delta H_m}{\text{PLA}_{100\%}} \times 100 [\%], \quad (1)$$

$$\chi_{cf} = \frac{\Delta H_m - |\Delta H_c|}{\text{PLA}_{100\%}} \times 100 [\%], \quad (2)$$

2.2.4. Thermogravimetric Analysis-Fourier-Transform Infrared Spectrometry (TGA-FTIR)

In the TGA-FTIR test, the two devices were connected so that the gas phases released in the TGA test travel through the sensors of the FTIR device. The gases went through a silicon tube; flow was maintained with nitrogen background gas. The FTIR test can determine the chemical composition of the gas from the TGA test. With this method, the composition of the gas can be determined across the whole temperature range. The TGA-FTIR measurements were performed with a TA Instruments Q5000 (New Castle, DE, USA) automatic sampling device. The measurement temperature range was 40–800 °C, the heating rate was 10 °C/min, the mass of the samples was between 1 mg and 4 mg and the tests were performed in nitrogen protective gas (25 mL/min) and with nitrogen measuring atmosphere (50 mL/min). The TGA device was connected to a Bruker Tensor 37 FTIR (Billerica, MA, USA) device. Gas was released at different temperatures in the case of the different CBAs and the spectrum was evaluated at the maximum of effective gas generation in each case (in the case of Tracel3170 it was 190 °C, in the case of Tracel4200 it was 175 °C, in the case of Luv_9537 it was 157 °C, while in the case of Hyd_3168 it was 232 °C). We took into account the effective gases which are generated below manufacturing temperature.

2.2.5. Thermogravimetric Analysis Performed in Isothermal Conditions

TGA measurements were performed with a TA Instruments Q500 (New Castle, DE, USA) automatic sampling device. The measurement temperature was 190 °C, the heating rate was 100 °C/min, the mass of the samples was between 1 mg and 4 mg and the tests were performed in nitrogen protective gas (40 mL/min) and with industrial air measuring atmosphere (60 mL/min). These conditions are closer to those in an extruder. The isothermal temperature was chosen to be 190 °C because this is a usual processing temperature during the extrusion of PLA. The background gas was chosen to be air, because the CBA may get into contact with air during the manufacturing process. The samples reached the isothermal 190 °C in 3 min and they were kept at this temperature for another 330 s.

2.2.6. Scanning Electron Microscopy (SEM)

Scanning electron micrographs were taken from fracture surfaces with a Jeol JSM-6380LA (Tokyo, Japan) SEM with an acceleration voltage of 10 kV. Prior to the test, the samples were sputter-coated with a gold/palladium alloy.

2.2.7. Foam Characterisation

The volume of foam structures was measured with a 10 mL glass cylinder (accuracy 0.1 cm³); the measuring medium was distilled water. Mass was measured with a Sartorius BP121S type balance (Göttingen, Germany). Its range is 120 g, its measuring accuracy is 0.1 mg and its resolution is 0.1 mg. Density was calculated according to Equation (3).

$$\rho_{\text{foam}} = \frac{m_{\text{foam}}}{V_{\text{foam}}}, \quad (3)$$

Void fraction was calculated according to Equation (4) [24].

$$V_f = 1 - \frac{\rho_{\text{foam}}}{\rho_{\text{polymer}}}, \quad (4)$$

where V_f [-] is void fraction, ρ_{foam} is the density of the foamed polymer and ρ_{polymer} is the density of unfoamed polymer.

Cell population density was calculated based on the SEM images, according to Equation (5), where n is the number of cells counted in the recorded image, A [cm²] is the cross section area of the sample, M [-] is the magnification factor and ER [-] is the expansion ratio [24].

$$N_c = \left(\frac{n * M^2}{A} \right)^{\frac{3}{2}} \times \frac{1}{1 - V_f}, \quad (5)$$

The expansion ratio was calculated with Equation (6), where ER is the rate of expansion, ρ_{foam} is the density of the foamed polymer, ρ_{polymer} is the density of unfoamed polymer and V_f is the void fraction [16].

$$ER = \frac{\rho_{\text{polymer}}}{\rho_{\text{foam}}} = \frac{1}{1 - V_f}, \quad (6)$$

2.2.8. Measuring Foam Strength

Foam compressive strength tests were performed with a Zwick Z005 (Ulm, Germany) universal testing machine (in compression mode). A Mess & Regeltechnik KAP-TC (Dresden, Germany) type load cell was used (measuring range 0–5000 N, preload 1 N). The measurement speed applied was 2 mm/min. The specimens were cylindrical, with a diameter of 3 mm and a height of 10 mm (Figure 2). The test was continued until a deformation of 10% was reached. Five samples were tested and the average of the results was taken. Foam compressive strength was calculated in accordance with Equation (7).

$$\sigma_{10\%} = \frac{F_{10\%}}{A_{\text{foam}}}, \quad (7)$$

where compressive strength [MPa] is the compression strength at 10% deformation, $F_{10\%}$ [N] is the force at 10% deformation and A_{foam} [mm²] is the cross-sectional area of the foam specimen.

Extrusion foaming was carried out with a Teach-line ZK25T (Collin GmbH, Ebersberg, Germany) twin-screw extruder (screw diameter: 25 mm, L/D = 24). The temperature profiles of the five zones starting from the hopper were 155 °C, 160 °C, 175 °C, 190 °C and 190 °C. Screw speed was 10 revolutions per minute, the residence time of the polymer was 330 s, pressure drop [MPa] was calculated according to Equation (8), where p_{melt} [MPa] is the pressure that we measured during extrusion in the die, p_{atm} [MPa] is the standard atmospheric pressure, 0,1 MPa. The extrusion die was a rod type with a circular cross section and with a nominal diameter of 3 mm. All foaming agents were added to the PLA granules during extrusion in an amount of 2 wt%, by dry mixing. Prior to manufacturing, the PLA granules were dried at 80 °C for 6 h in a WGL-45B type drying oven.

$$\text{Pressure drop} = p_{\text{melt}} - p_{\text{atm}} \quad (8)$$

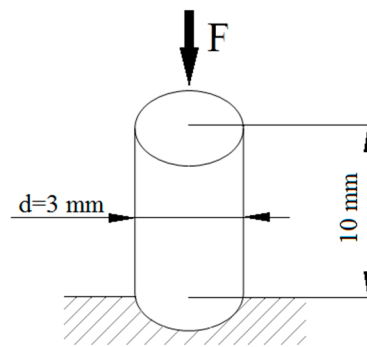


Figure 2. Measurement layout of measuring foam strength.

3. Results of the Investigation of the Foaming Agents

3.1. The Thermal and Morphological Properties of CBAs, TGA, TGA-FTIR, DSC

First, we examined the decomposition temperature ranges of chemical foaming agents by TGA. The test showed the mass fraction of the CBAs, the fraction of the gas producer useful from the aspect of foaming and what is the proportion of carrier polymer and other residual materials. The samples were measured with two background gases, so it was possible to compare the processes occurring in the different media. We used a nitrogen (N_2) atmosphere to get measurement results from an inert atmosphere, while air was used because that is what is present during extrusion; therefore, the measurement approximates real-life extrusion better. Figure 3 shows that the decomposition of CBAs occurred in several steps. In the case of Luv_9537, mass reduction starts at $136\text{ }^\circ\text{C}$, this CBA is followed by Tracel4200, then Tracel3170. While in the case of the exothermic Tracel3170, mass reduction occurs in one step up to $200\text{ }^\circ\text{C}$, the endothermic Tracel4200 and Luv_9537 exhibit mass reduction in two steps. Between $150\text{--}250\text{ }^\circ\text{C}$ during the thermal decomposition of CBAs probably effective gases, taking an active part in foaming are released, above this temperature it is likely that the carrier materials decompose. In the case of Hyd_3168 and Luv_9537, a great reduction of mass can be observed at $300\text{ }^\circ\text{C}$ and $444\text{ }^\circ\text{C}$, while in the case of Tracel3170 and 4200, an extended gradual decrease can be observed at low intensity. Comparing the same measurements in N_2 and air, we can conclude that gas formation occurs in the same temperature range. In air, the curve is continuously sloping, while in nitrogen the decomposition ranges separate; the degradation of the carrier polymer and the accompanying mass reduction only starts at around $400\text{ }^\circ\text{C}$. Table 2 contains the measurement results: the decomposition temperature ranges based on dTG and the percentage ratio of mass reduction at $190\text{ }^\circ\text{C}$. The data indicate that in the case of the investigated CBAs, in nitrogen and air atmosphere, at $190\text{ }^\circ\text{C}$, mass reduction was nearly the same. There is a greater difference only in the case of Tracel3170; in nitrogen mass reduction was 7.5%, while in air it was only 2.8%. The greatest mass reduction in nitrogen was observed in the case of Tracel3170 (7.5%), it is followed by Tracel4200 (6.9%), Luv_9537 (4.8%) and Hyd_3168 (0.1%). The data indicate that Hyd_3168 probably cannot produce a foam at $190\text{ }^\circ\text{C}$, the characteristic processing temperature of PLA. All four foaming agents produced residual mass at $800\text{ }^\circ\text{C}$, which is probably a nucleating agent.

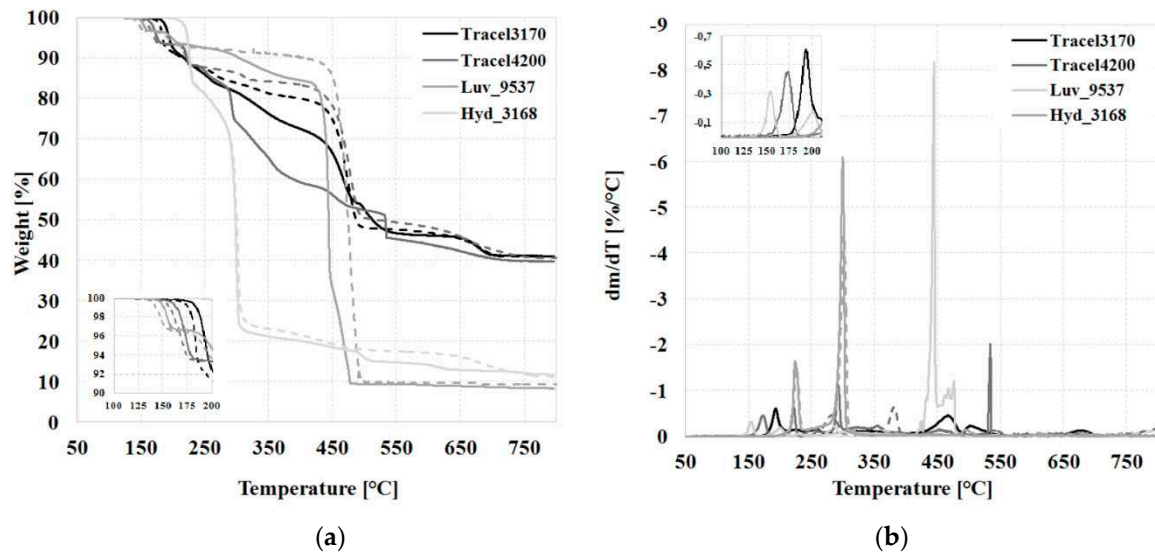


Figure 3. Thermogravimetric analysis (TGA) results of foaming agents in nitrogen and air (a) mass reduction as a function of temperature (50–800 °C), (b) the rate of mass reduction as a function of temperature (50–800 °C). The broken line indicates the nitrogen atmosphere, while the continuous line indicates air.

Table 2. The decomposition range of CBAs (dTG ranges relevant from the aspect of PLA extrusion processing) and mass reduction at 190 °C.

Sample	dTG Range	Mass Reduction	dTG Range	Mass Reduction at
	N ₂	at 190 °C N ₂	Air	190 °C Air
[-]	[°C]	[%]	[°C]	[%]
Tracel3170	145–239	7.5	147–212	2.8
Tracel4200	145–188, 204–245	6.9	147–187, 196–232	6.5
Hyd_3168	186–237	0.1	193–237	0.1
Luv_9537	136–168, 168–225	4.8	137–165, 174–214	3.9

We evaluated the gases released at the maximum intensity of decomposition with a TGA-FTIR measurement. The results can be seen in Figure 4. We determined the type of gases generated under the processing temperature (Table 3). The maximum intensity of gas generation in the case of the different CBAs: Tracel3170—183 °C, Tracel4200—168 °C, Luv_9537—147 °C, while in the case of Hyd_3168 there was no observable gas generation intensity maximum under 200 °C, the maximum occurred at 225 °C. Based on the spectrum measured by FTIR, in the case of Tracel3170, peaks indicating carbon dioxide have the highest intensity but carbon monoxide is also present with lower absorption. Also, a C=N bond appears as well, which indicates isocyanate ($\sim 2200\text{--}2350\text{ cm}^{-1}$), which is a typical decomposition product of azodicarbonamide. In the case of Tracel4200, a strong absorption carbon dioxide peak can be observed but no carbon monoxide. In the case of Luv_9537, the absorption wavelength of carbon dioxide can be observed. In the case of Hyd_3168, carbon dioxide appears as an effective gas but with a small intensity peak. It is important to note that the type of effective gas also has an effect on the final foam structure. CO₂ has higher solubility (20 wt%) in the PLA matrix compared to N₂ (2 wt%). As a result, CO₂ effectively lowers melt pressure during extrusion and increases the percentage of crystalline fraction [25]. The reaction range of CBAs was also analysed with a DSC test. Figure 5 below contains the measurement results.

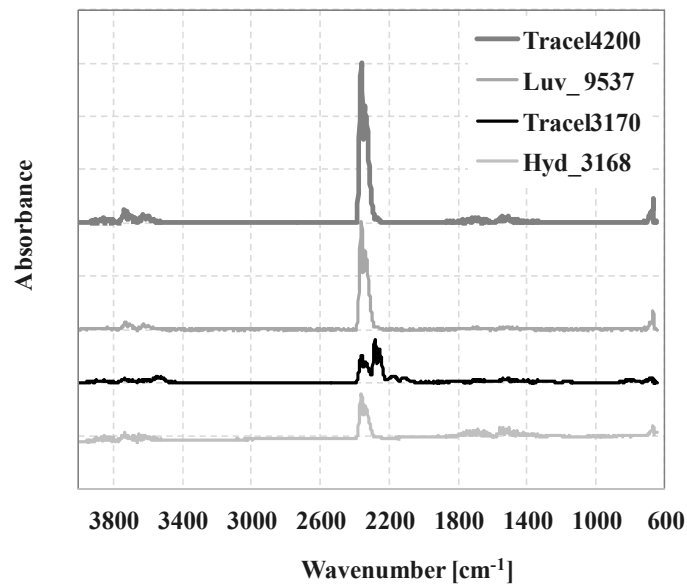


Figure 4. The Fourier transform infrared (FTIR) spectrum of foaming agents (in the 600–4000 cm⁻¹ range).

Table 3. The results of the TGA-FTIR measurement (10 °C/min, nitrogen measuring atmosphere).

Foaming Agent	Absorbance Maximums [-]		Type of Gas Generated
	Wave Number [cm ⁻¹]	Temperature [°C]	
Tracel3170	600–750, 2250–2350, 3600–3750	183	CO ₂
	2050–2250	183	CO
	750–1250, 1450–1800, 3200–3500	183	NH ₃
Tracel4200	600–750, 2250–2350, 3600–3750	168	CO ₂
	1600–1700, 3500–3700	168	H ₂ O
Luv_9537	2050–2250	147	CO
	600–750, 2250–2350, 3600–3750	147	CO ₂
Hyd_3168	2050–2250	225	CO
	600–750, 2250–2350, 3600–3750	225	CO ₂

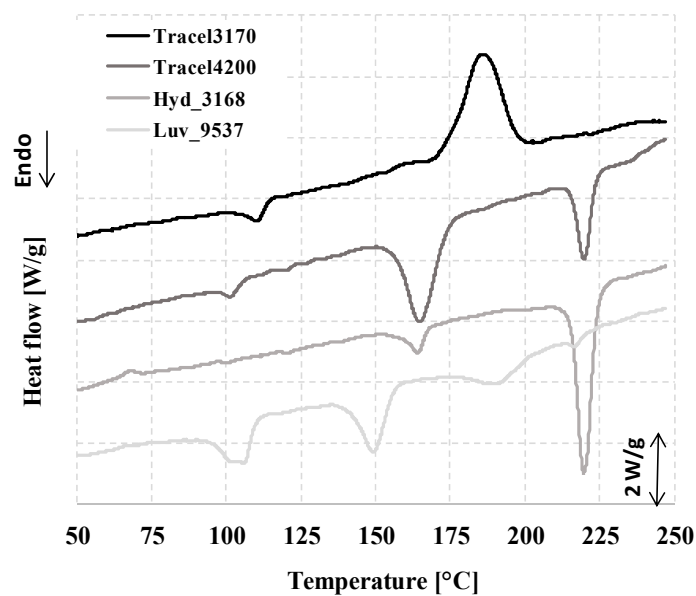


Figure 5. Differential scanning calorimetry (DSC) results of foaming agents (50–250°C, first heating, 10 °C/min).

We compared the absorbance spectrum of generated effective gases with the intensity peaks of the spectra of materials in the IR database of the National Institute of Standards and Technology [26].

Figure 5 shows that Tracel3170 has an exothermic conversion peak, while in the case of Tracel4200, Luv_9537 and Hyd_3168, more endothermic reaction occurred. The conversion temperatures measured by DSC can be compared to the temperature ranges measured by TGA and this provides more accurate information concerning the temperature range of the decomposition process. Table 4 contains these data. The initial chemical change temperature of DSC is nearly the same as the beginning of the decomposition range measured by TGA but the end of the decomposition range (according to dTG) falls a little after the end of the changing temperature range registered by DSC. This is because the DSC data describe the changing process of the foaming agent and only the beginning part of this process is the same as TGA. TGA, on the other hand, does not show the energy change before and after the start of decomposition; it only registers the mass reduction effect of the decomposition product released in the gas phase, which continues after the reaction, as well.

Table 4. Comparison of decomposition processes registered with DSC and TGA tests.

Sample	Decomposition Range According to dTG *	Decomposition Range According to dTG *	State Change **
	N ₂	Air	N ₂
[-]	[°C]	[°C]	[°C]
Tracel3170	145–239	147–212	165–200
Tracel4200	145–188, 204–245	147–187, 196–232	150–180, 210–225
Hyd_3168	186–237	193–237	153–169, 208–229
Luv_9537	136–168, 168–225	137–165, 174–214	136–160, 175–200

* TGA measurement, ** DSC measurement.

3.2. Isothermal Thermogravimetric Analysis

Foaming agents have to produce effective gas at the processing temperature of PLA. In the previous tests, a constant heating rate was used (10 °C/min) but thermal conditions are different during actual manufacturing. Therefore, as a next step, we investigated decomposition by TGA at a constant temperature, 190 °C. Figure 6a,b show the results of the isothermal TGA test. Figure 5 shows that as a result of constant temperature, decomposition also occurs. For evaluation, however, the results must be compared to the previous results so that any possible differences could be seen. Table 5 contains the numerical data. Comparing the TGA and isothermal TGA measurement data, we can draw conclusions about the behaviour of foaming agents. There is no big difference between the results of the two types of measurement but mass reduction was greater in the case of the isothermal process. The biggest difference was observed in the case of Tracel3170, where isothermal mass reduction was 4.9%, which is 2.1% greater than in the case of a constant heating rate. There is a difference in the case of the other three foaming agents too but it is smaller.

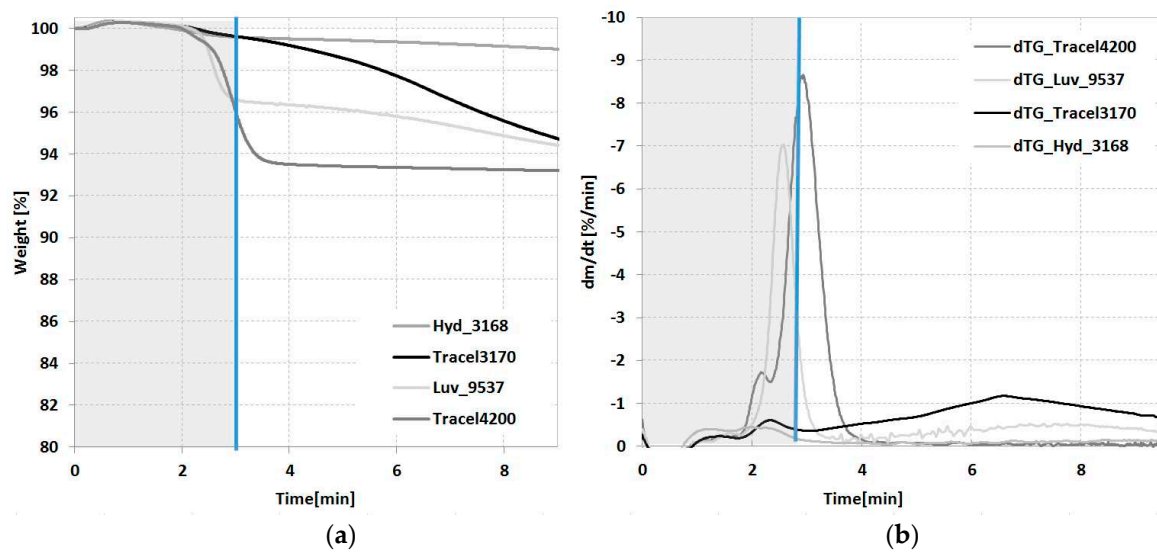


Figure 6. TGA decomposition of foaming agents at 190 °C in isothermal conditions in a measuring atmosphere of air (a) mass reduction as a function of time, (b) dTG as a function of time (the blue line shows the moment of reaching 190 °C).

Table 5. The decomposition range of CBAs at an isothermal temperature.

Sample	Mass Reduction	
	(10 °C/min, 190 °C) Air	(Isothermal, 190 °C, 330 s) Air
[-]	[%]	[%]
Tracel3170	2.8	4.9
Tracel4200	6.5	6.8
Luv_9537	3.9	5.4
Hyd_3168	0.1	0.9

4. Chemical Foaming of Poly(Lactic Acid)

Foaming, Processing

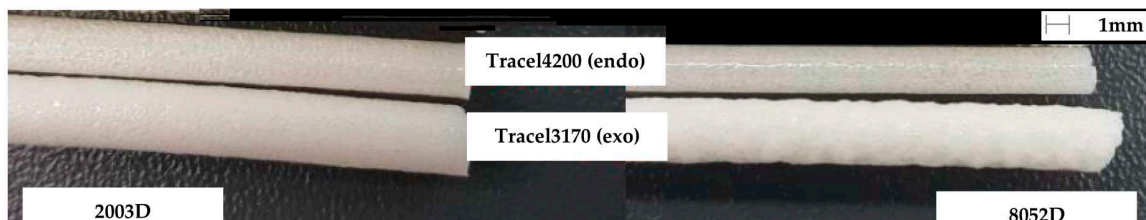
The temperature parameters of extrusion foaming were selected based on the typical processing temperature of PLA; technical datasheets recommend processing at 190–200 °C. Table 6 contains the designations of the manufactured specimens and Table 7 contains the manufacturing parameters. We experienced during manufacturing that in the case of 8052_4200 and 2003_4200, melt pressure decreased drastically from the initial 74 to 43 bar and the viscosity of the melt changed considerably when it exited the die and in the case of 8052_Hyd_3168 and 2003_Hyd_3168, we did not see signs of successful cell formation in the material flow exiting the die – the sample continued to be transparent, only its colour became whiter. The extruded reference rod is basically smooth and transparent. Figure 7 shows that in the case of 8052_4200, 2003_4200 and 8052_3170, 2003_3170, foaming produced a different surface on the specimens. Tracel4200 produced a surface similar to PLA but with a little whitening and the cells are visible. Tracel3170 produced a coarser surface and the cells can be felt on the surface. Although Tracel3170 is an AZO type foaming agent, 8052_3170, 2003_3170 show only a very small yellowish tint. Foaming agents that can produce effective gases at 190 °C reduced melt viscosity during extrusion.

Table 6. The designation of the samples and their recipes.

Sample Code	PLA Used	CBA Used	CBA Dosing	Note
[-]	[Type]	[Type]	[wt%]	[-]
2003_ref	2003D	-	0	extruded once
8052_ref	8052D	-	0	extruded once
2003_3170	2003D	Tracel3170	2	-
8052_3170	8052D	Tracel3170	2	-
2003_4200	2003D	Tracel4200	2	-
8052_4200	8052D	Tracel4200	2	-
2003_Luv_9537	2003D	Luv_9537	2	-
8052_Luv_9537	8052D	Luv_9537	2	-
2003_Hyd_3168	2003D	Hyd_3168	2	-
8052_Hyd_3168	8052D	Hyd_3168	2	-

Table 7. Manufacturing parameters.

Sample Code	T _{melt}	P _{melt}	Pressure Drop
-	°C	bar	MPa
2003_ref	196	74	7.3
8052_ref	196	43	4.2
2003_3170	196	32	3.2
8052_3170	195	21	2.0
2003_4200	196	14	1.3
8052_4200	196	13	1.2
2003_Luv_9537	196	18	1.7
8052_Luv_9537	196	34	3.3
2003_Hyd_3168	197	56	5.5
8052_Hyd_3168	196	46	4.5

**Figure 7.** The surface of 2003_3170, 2003_4200 and 8052_3170, 8052_4200 foam structures manufactured at 190 °C.

5. Results of the Foamed Poly(Lactic Acid)

5.1. Scanning Electron Microscopy

We evaluated the cell structure of the manufactured foam samples based on scanning electron microscope (SEM) images. Figure 8 shows characteristic SEM images of the foam structure. They indicate that foaming took place in the case of both polymer matrices and all three foaming agents (Tracel3170, Tracel4200 and Luv_9537). Hyd_3168 applied at 190 °C could not form a cell structure in the case of either PLA matrix. This corresponds to the TGA results, which showed that Hyd_3168 could not form effective gas at 190 °C in 330 s (the modelled extrusion time) and therefore a cell structure could not form.

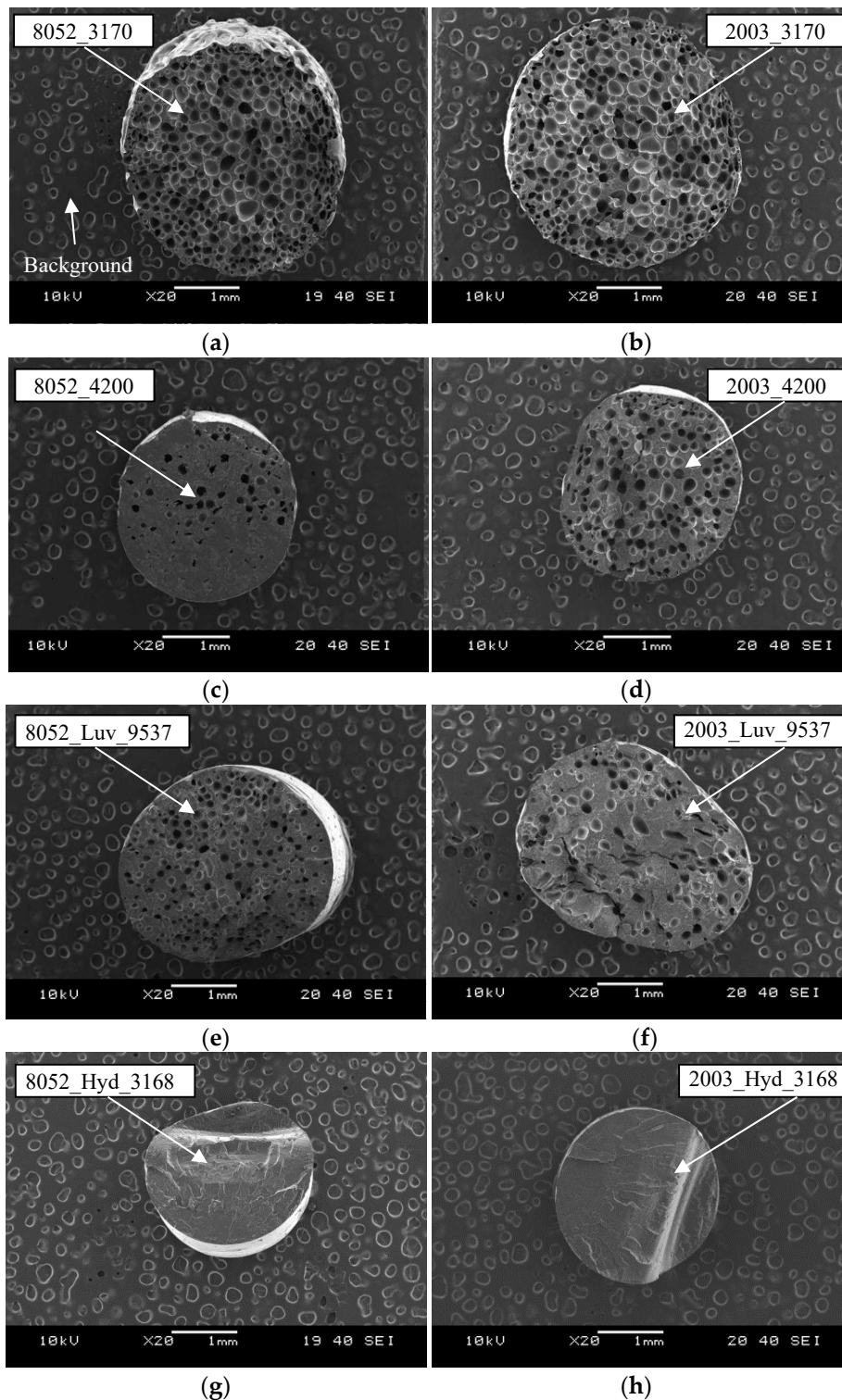


Figure 8. Scanning electron microscopy (SEM) images of samples foamed with different foaming agents (manufactured at 190 °C) (a) 8052_3170, (b) a 2003_3170, (c) 8052_4200, (d) 2003_4200, (e) 8052_Luv_9537, (f) a 2003_Luv_9537, (g) 8052_Hyd_3168, (h) 2003_Hyd_3168 20× magnification.

5.2. The Morphology of Foam Structures

We graded foam structures by cell population density, expansion, void fraction and density. The results can be found in Figures 9 and 10. The exothermic Tracel3170 produced more cells in unit volume in the case of the 8052_3170 recipe recommended for foaming (4.82×10^5 cells/cm³) than in

the case of 2003_3170 (4.17×10^5 cells/cm³). The 8052D polymer not only produces a higher number of cells but the expansion of the cells is also higher, 2.36, as opposed 2.18 in the case the 2003_3170. As a result, density with 8052_3170 was lower, 0.53 g/cm³, while in the case of 2003_3170, it was 0.57 g/cm³. This means that a void fraction of 57.61% was achieved in the case of the 8052_3170 recipe (considering that the density of PLA is 1.24 g/cm³). The good results can be attributed to the nucleating agent Tracel3170 contained based on the manufacturer’s data and the TGA results (residual material content of 40.96% at 800 °C).

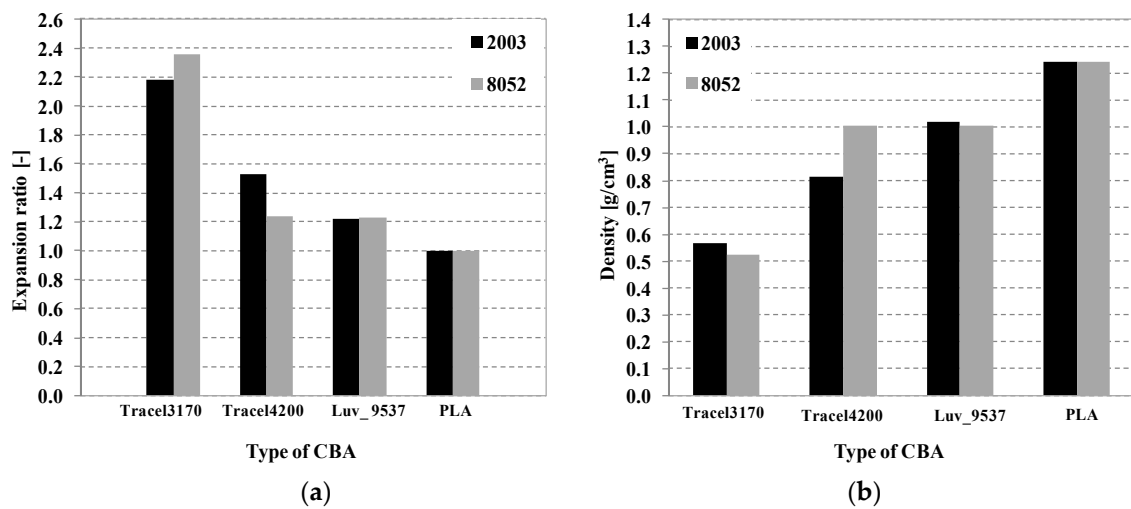


Figure 9. Foamed sample (a) expansion values (b) density values (manufacturing temperature 190 °C).

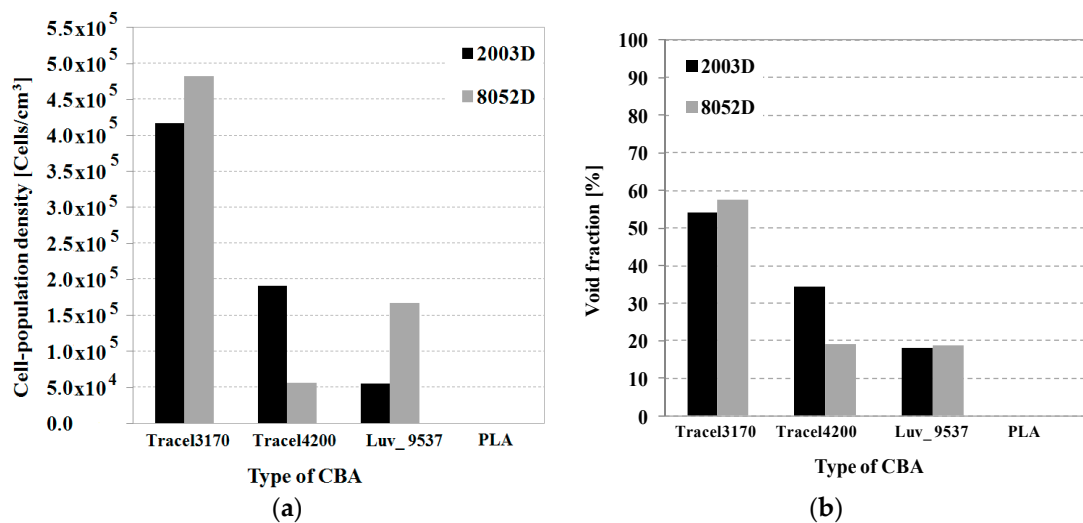


Figure 10. (a) Cell population density and (b) porosity in the case of the different foaming agent types (manufacturing temperature 190 °C).

The endothermic Tracel4200 produced fewer cells per unit volume in the case of the 8052_4200 recipe recommended for foaming (5.58×10^4 cells/cm³) than in the case of the 2003_4200 recipe (1.91×10^5 cells/cm³). In the case of the 2003D the expansion of the cells is also better, 1.53, as opposed to 1.24 in the case of the 8052_4200. This is because the decomposition products of Tracel4200 include water, which probably hydrolysed the PLA, causing its melt pressure, viscosity and melt strength to decrease during the foaming process. Since the M_w of 8052D is lower (153,235 Da) than that of 2003D (180,477 Da), it resisted degradation by hydrolysis and produced better cell population density and expansion than the 8052D type PLA. The density of foam structures manufactured with Tracel4200

was 1.00 g/cm³ in the case of the 8052_4200, while 0.81 g/cm³ in the case of the 2003_4200, which is less than the density reduction achieved with Tracel3170.

The endothermic Luv_9537 foaming agent produced more cells per unit volume in the case of the 8052_Luv_9537 recipe recommended for foaming (1.67×10^5 cells/cm³) than in the case of the 2003_Luv_9537 recipe (5.51×10^4 cells/cm³). Although the cells expanded, expansion in the case of the 2003D polymer was 1.22 and in the case of the 8052_Luv_9537 recipe, it was 1.23, which is quite little in both cases. The SEM images show that the size and shape of the cells in the case of the 8052_Luv_9537 are not homogeneous. The densities of PLA foams made with the Luv_9537 foaming agent are about 1 g/cm³ in both cases. In the case of 2003_Luv_9537, density is 1.02 g/cm³, while in the case of 8052_Luv_9537, it is 1.01 g/cm³.

We did not characterize the 2003_Hyd_3168 and 8052_Hyd_3168 recipes with the methods used for the characterization of foam structures, since no foam structure was formed during manufacturing. Only the PLA matrix formed a blend with the carrier of the CBA without the effective gases being able to form a gas phase and nucleate cells.

In the case of exothermic foaming, PLA foamed to a much greater degree than in the case of endothermic foaming and so densities were lower. This is due to the type of the endothermic reaction products on the one hand and to the effective gas formation temperature ranges unfavourable for PLA and the foaming agent fraction of the CBA granules.

5.3. Differential Scanning Calorimetry

We examined the morphology that formed after foaming process, using differential scanning calorimetry, the results of which can be seen in Figure 11 and Table 8. Figure 11 shows the DSC curves of the single-processed reference poly(lactic acid) (extruded granules, processed similarly to foamed samples 2003_ref and 8052_ref) and the foamed samples in the case of the first heating curve. In the case of foams manufactured with the same processing conditions, the glass transition temperature of the polymer (T_g), which is the first registered endothermic change in the DSC curve, was not different from the reference value in the case of the Tracel4200 foaming agent and the 8052_3170 recipe. On the other hand, in the case of the other foaming agents T_g decreased by 2–4 °C (Table 8). A change in the second registered heat flow is the exothermic phenomenon of cold crystallization, which, in the case of foam structures, shifts considerably to lower temperatures. The foaming agent causes cold crystallization to happen at a much lower temperature than in the case of neat PLA. The second, bigger endothermic peak is the crystalline fraction melting range. It can be observed that the extruded foam samples are capable of cold crystallization during the DSC test, which is an exothermic reaction. This is because after processing, due to fast cooling, the crystalline fraction cannot fully form, since the molecular chains do not have time to get ordered. During the DSC test, due to the relatively slow temperature rise (5 °C/min), the molecular chains can become more ordered, which is accompanied by the release of heat. These crystalline fractions melt later, at a higher temperature and the polymer melts. In the case of 8052D, two crystalline melting peaks can be observed. Frackowiak et al. [27] provided the explanation that crystals with lower melting temperatures are smaller and formed during cold crystallization, while, crystal types with a higher melting temperature formed during the primary crystallization process, therefore, in our case, they are created by the technology. Therefore, foaming agents influence the crystalline structure that forms in the polymer. The crystalline melting range has two peaks and is composed of two different crystalline types: the α and α' types. The α' type has a lower melting temperature, while the α type has a higher melting temperature and is also thermodynamically more stable. The range between the melting of the two phases is called α' – α phase transition [27]. The crystalline fraction forming during manufacturing is typically low, due to the cooling of the polymer in open air (<5%). The foam structure with the highest population density and highest expansion has the highest crystalline fraction from manufacturing (4.3%). Crystalline fraction was typically higher than that of reference PLA; the nucleating agents in the CBAs probably had a beneficial effect on the forming of crystalline nuclei. Thus, the foaming agent affected the crystalline

state and structure of the samples and also their thermal properties. In the presence of the foaming agent, transition temperatures typically shifted to lower temperatures compared to the reference poly(lactic acid).

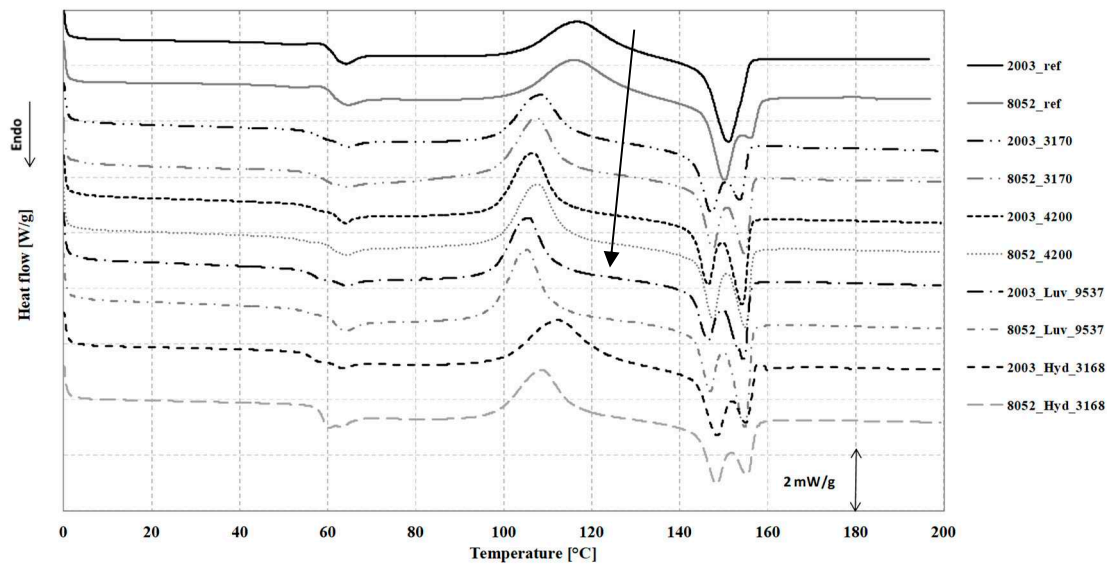


Figure 11. The DSC curves of reference PLA and foamed samples (1st heat-up, 5 °C/min).

Table 8. DSC results of foamed samples and unfoamed, extruded PLA (1st heat-up, 5 °C/min).

Type of Sample	T _g	T _{c1}	ΔH _c	T _{m1}	T _{m2}	ΔH _m	χ _c	χ _{cf}
[-]	[°C]	[°C]	[J/g]	[°C]	[°C]	[J/g]	[%]	[%]
2003_ref	59.6	116.7	23.8	151.1	-	26.4	28.4	6.9
8052_ref	59.2	115.9	25.2	150.3	-	28.8	31	3.1
2003_3170	57.5	108.4	26.5	147.3	153.8	28.1	30.2	1.7
8052_3170	59.6	107.5	27.4	147.6	154.8	31.4	33.8	4.3
2003_4200	59.3	114.5	29.5	147.2	154.2	32.2	34.6	2.9
8052_4200	59.6	107.9	29.3	143.7	154.9	30.5	32.8	1.3
2003_Luv_9537	57.2	105.6	28.8	146.4	154.4	30.1	32.4	1.4
8052_Luv_9537	55.4	105.4	33.7	147.1	154.8	34.5	37.1	0.9
2003_Hyd_3168	56.2	112.3	29.6	148.5	155.2	31	33.3	1.5
8052_Hyd_3168	57.5	108.3	27.4	148.5	155.5	28.3	30.4	1.0

5.4. Foam Strength

Foam samples were finally tested mechanically. A widely used test of foamed products is the foam strength test. We only performed the test on samples deemed acceptable (void fraction >40%), that is on 2003_3170 and 8052_3170 samples. Figure 12 shows the measurement curves selected as typical. The shape of the curves is characteristically the same as that of other known foam strength curves coincides. At initial loading, in the linear section, deformation is elastic, then a peak follows, which corresponds to “yield strength.” In elastic deformation, the cells take up the load, then they are restored to their original state when loading stops. At the inflexion part, however, the cells are deformed and damaged. The straight section (the section after the inflexion point) appeared in the curve of every specimen within the 10% deformation limit, that is, each specimen suffered permanent deformation. In the case of 2003_3170, it is 22.8 ± 0.6 MPa, while in the case of 8052_3170, it is 22.4 ± 0.7 MPa. There was no significant difference between the compression strength values of foams produced with Tracel3170 and the two different types of PLA; the compression strengths and standard deviations are nearly the same. The aim was to create biodegradable hard foams with the use of commercially available CBAs. Compressive strength is higher, compared physically foamed PLA

in the literature [21]. The results should be considered a reference value when later modified foam structures are developed later.

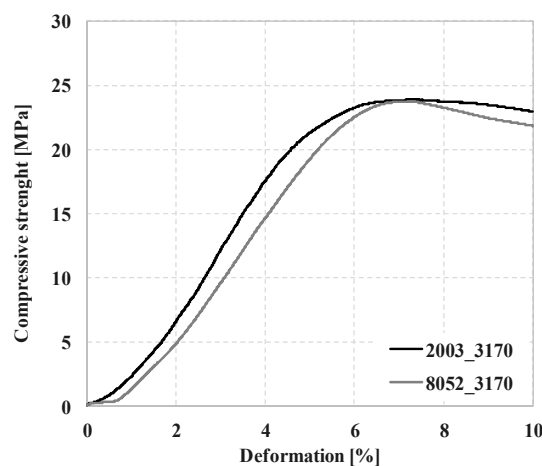


Figure 12. Compression strength deformation diagram in the case of 2003_3170 and 8052_3170 recipes.

6. Conclusions

We comprehensively examined chemical blowing agents and determined their properties. Then we foamed poly(lactic acid) with endothermic and exothermic foaming agents recommended for polyester and an endothermic foaming agent specially recommended for poly(lactic acid). We examined the cell population density, cell expansion, void fraction, density, morphology and mechanical properties of the manufactured foams. Our results indicate that the exothermic azodicarbonamide foaming agent (Tracel IM 3170 MS) added to 8052D PLA in 2 wt% is a very promising foaming agent at the processing temperature of 190 °C. The cell population density of such foams is 4.82×10^5 cells/cm³, their expansion is 2.36, their density is 0.53 g/cm³, their void fraction is 57.61% and their compression strength is 22.4 ± 0.7 MPa.

Author Contributions: Conceptualization, Á.K.; methodology, Á.K. and K.L.; formal analysis, Á.K. and K.L.; investigation, D.R. and K.L.; writing—original draft preparation, Á.K. and K.L.; writing—review and editing, Á.K.

Funding:



Supported by the ÚNKP-17-4-III New National Excellence Program of the Ministry of Human Capacities. This research was also supported by The National Research, Development and Innovation Office (NVKP_16-1-2016-0012).

Acknowledgments: The author would like to thank Tim Stoesser, Department of Chemistry, Oxford University, Oxford, UK for his help with the GPC measurements.

Conflicts of Interest: The authors declare no conflict of interest. The funders had no role in the design of the study; in the collection, analyses, or interpretation of data; in the writing of the manuscript, or in the decision to publish the results.

References

- Jost, V. Packaging related properties of commercially available biopolymers—An overview of the status quo. *Express Polym. Lett.* **2018**, *12*, 429–435. [[CrossRef](#)]
- Aeschelmann, F.; Carus, M. Biobased Building Blocks and Polymers in the World: Capacities, Production, and Applications—Status Quo and Trends Towards 2020. In *Industrial Biotechnology*; nova-Institut GmbH: Huerth, Germany, 2015; p. 154.
- Di Maio, E.; Kiran, E. Foaming of polymers with supercritical fluids and perspectives on the current knowledge gaps and challenges. *J. Supercrit. Fluids* **2018**, *134*, 157–166. [[CrossRef](#)]

4. Wypych, G. *Handbook of Foaming and Blowing Agents*; ChemTec Publishing: Toronto, ON, Canada, 2017; Volume 1.
5. Raps, D.; Hossieny, N.; Park, C.B.; Altstädt, V. Past and present developments in polymer bead foams and bead foaming technology. *Polymer* **2015**, *56*, 5–19. [[CrossRef](#)]
6. Orbulov, I.; Katona, B. Structural Damages in Syntactic Metal Foams Caused by Monotone or Cyclic Compression. *Periodica Polytech. Mech. Eng.* **2017**, *61*, 146–152.
7. Okolieocha, C.; Raps, D.; Subramaniam, K.; Altstädt, V. Microcellular to nanocellular polymer foams: Progress (2004–2015) and future directions—A review. *Eur. Polym. J.* **2015**, *73*, 500–519. [[CrossRef](#)]
8. Lee, S.-T.; Park, C.B.; Ramesh, N.S. *Polymeric Foams: Science and Technology*; Taylor and Francis Groupe: Boca Raton, FL, USA, 2007.
9. Lee, S.-T. *Foam Extrusion*, 2nd ed.; CRC Press: Boca Raton, FL, USA, 2014.
10. Lee, S.-T. *Polymer Foams Innovations in Processes, Technologies, and Products*; CRC Press: Boca Raton, FL, USA, 2017.
11. Khemani, K.C. *Polymeric Foams Science and Technology*; American Chemical Society: Washington, DC, USA, 1997.
12. Eaves, D. *Polymer Foams Trends in Use and Technology*; Rapra Technology Limited: Shawbury, UK, 2001.
13. Ludwiczak, J.; Kozłowski, M. Foaming of Polylactide in the Presence of Chain Extender. *J. Polym. Environ.* **2014**, *23*, 137. [[CrossRef](#)]
14. Julien, J.M.; Quantin, J.-C.; Bénézét, J.-C.; Bergeret, A.; Lacrampe, M.F.; Krawczak, P. Chemical foaming extrusion of poly(lactic acid) with chain-extendors: Physical and morphological characterizations. *Eur. Polym. J.* **2015**, *67*, 40–49. [[CrossRef](#)]
15. Julien, J.-M.; Bénézét, J.-C.; Lafranche, E.; Quantin, J.-C.; Bergeret, A.; Lacrampe, M.-F.; Krawczak, P. Development of poly(lactic acid) cellular materials: Physical and morphological characterizations. *Polymer* **2012**, *53*, 5885–5895. [[CrossRef](#)]
16. Matuana, M.L.; Faruk, O.; Diaz, C.A. Cell morphology of extrusion foamed poly(lactic acid) using endothermic chemical foaming agent. *Bioresour. Technol.* **2009**, *100*, 5947–5954. [[CrossRef](#)] [[PubMed](#)]
17. *Tramaco Vertrieb und Verarbeitung von Chemieprodukten GmbH*; Chemical Foaming Agents: Pinneberg, Germany, 2014.
18. Yuan, H.; Liu, Z.; Ren, J. Preparation, Characterization, and Foaming Behavior of Poly(lactic acid)/Poly(butylene adipate-co-butylene terephthalate) Blend. *Polym. Eng. Sci.* **2009**, *49*, 1004–1012. [[CrossRef](#)]
19. Niaounakis, M. *Biopolymers: Applications and Trends*; PDL Handbook Series; William Andrew: Chadds Ford, PA, USA, 2015.
20. Nofar, M.; Park, C.B. Poly (lactic acid) foaming. *Prog. Polym. Sci.* **2014**, *39*, 1721–1741. [[CrossRef](#)]
21. Bocz, K.; Tábi, T.; Vadas, D.; Sauceau, M.; Fages, J.; Marosi, G. Characterisation of natural fibre reinforced PLA foams prepared by supercritical CO₂ assisted extrusion. *Express Polym. Lett.* **2016**, *10*, 3144. [[CrossRef](#)]
22. Wypych, G. *Databook of Blowing and Auxiliary Agent*; ChemTec Publishing: Toronto, ON, Canada, 2016.
23. Tábi, T.; Hajba, S.; Kovács, J.G. Effect of crystalline forms (α' and α) of poly(lactic acid) on its mechanical, thermo-mechanical, heat deflection temperature and creep properties. *Eur. Polym. J.* **2016**, *82*, 232–243. [[CrossRef](#)]
24. Xu, X.; Park, C.B.; Xu, D.; Pop-Iliev, R. Effects of Die Geometry on Cell Nucleation of PS Foams Blown With CO₂. *Polym. Eng. Sci.* **2003**, *43*, 1378–1390. [[CrossRef](#)]
25. Li, G.; Li, H.; Turng, L.S.; Gong, S.; Zhang, C. Measurement of gas solubility and diffusivity in polylactide. *Fluid Phase Equilib.* **2006**, *246*, 158–166. [[CrossRef](#)]
26. National Institute of Standards and Technology IR Database. Available online: <https://webbook.nist.gov/chemistry> (accessed on 15 December 2017).
27. Frackowiak, S.; Ludwiczak, J.; Leluk, K.; Orzechowski, K.; Kozłowski, M. Foamed poly(lactic acid) composites with carbonaceous fillers for electromagnetic shielding. *Mater. Des.* **2015**, *65*, 749–756. [[CrossRef](#)]

